Research paper

Porous Nd-doped In$_2$O$_3$ nanotubes with excellent formaldehyde sensing properties

Xuesong Wang, Jinbao Zhang, Yue He, Lianyuan Wang, Li Liu *, Han Wang, Xuexin Guo, Hongwei Lian

State Key Laboratory of Superhard Materials, College of Physics, Jilin University, Changchun 130012, PR China

ARTICLE INFO

ABSTRACT

Pure and Nd-doped porous In$_2$O$_3$ nanotubes have been successfully synthesized by single-capillary electrospinning method. The SEM images displays the novel structure of Nd-doped In$_2$O$_3$ which has pores distributed on the surface of nanotubes. The subsequent test results demonstrate that Nd-doped porous In$_2$O$_3$ nanotubes possess excellent gas-sensing properties to formaldehyde. The response of Nd-doped porous In$_2$O$_3$ nanotubes to 100 ppm formaldehyde is 44.6 at the optimum operating temperature of 240 °C, which is 3.6 times larger than that of pure porous In$_2$O$_3$ nanotubes (12.5), and the response and recovery times to 100 ppm formaldehyde are 15 and 50 s, respectively.

1. Introduction

For many years, semiconducting oxides have been widely used in many fields such as lithium-ion batteries [1], photosensitization [2], and gas sensors [3]. Gas sensors based on semiconducting oxides have received widely attentions which get benefit from their low cost, easy fabrication and portability [4]. Semiconducting oxide gas sensors can be used to detect toxic and inflammable gases such as formaldehyde and hydrogen [5,6]. However, there are some drawbacks which limit their applications including low sensitivity and poor selectivity [7]. Numerous studies have been undertaken to solve these problems. At present, increasing the surface-to-volume ratio and doping other elements are effective solutions to resolve these limitations [8,9]. For instance, Huang et al. demonstrated that In$_2$O$_3$-doped ZnO nanotubes show excellent ethanol-sensing characteristics [10]. Han et al. investigated the methanol gas-sensing performance of Ce-doped In$_2$O$_3$ porous nanospheres prepared by hydrothermal method [11].

In$_2$O$_3$ is an n-type semiconductor, which has been widely used due to its stable and nontoxic characteristics [12]. In recent years, various nanostructures of In$_2$O$_3$ such as nanoparticles [13], nanofibers [14], nanorods [15] and nanotubes [16] have been synthesized and applied to the field of gas sensors. However, porous In$_2$O$_3$ nanotube structure has rarely been reported. Previous studies have demonstrated that porosity plays a vital role in the application of semiconducting metal oxides as gas sensors [17]. Apart from

exhibiting high sensitivities due to large specific surface areas, sensors with well-defined porosity offer powerful opportunities with respect to selectivity, self-diagnosis, low operation temperatures or long-term stability [18,19]. However, the sensitivity of pure In$_2$O$_3$ nanotube gas sensors still needs to be improved. Many studies have been conducted to improve the sensing properties by doping other elements [20,21]. Rare-earth modified oxide compounds have been extensively studied in the field of gas sensors over the past decades due to their particular characteristics [22]. Nd is a kind of rare earth elements which owns the same nature with other rare earth elements. However, the studies on Nd-doped porous In$_2$O$_3$ nanotube gas sensors are quite rare.

In this paper, pure and Nd-doped porous In$_2$O$_3$ nanotubes are successfully obtained via the single-nozzle electrospinning and calcination methods. This novel nanostructure possesses a larger specific surface area that enhances its gas sensitivity. Moreover, the gas-sensing properties of the as-synthesized materials to formaldehyde are also investigated. The results show that the gas-sensing properties of porous In$_2$O$_3$ nanotubes have been enhanced significantly by doping Nd.

2. Experimental

2.1. Synthesis and characterization of materials

All chemical reagents were of analytical grade and used without further purification. Poly (vinylpyrrolidone) (PVP, M_w = 1 300 000) was obtained from Sigma-Aldrich (USA). In(NO$_3$)$_3$ (99.99%), Nd (NO$_3$)$_3$·6H$_2$O (99.99%), N,N-dimethylformamide (DMF ⩾ 99.5%),

---

and ethanol ($\geqslant$99.7%) were purchased from Aladdin (Shanghai, China).

Pure and Nd-doped porous In_2O_3 nanotubes were synthesized via an electrospinning method. 0.4 g of $In(NO_3)_3$ and 0.0358 g of $Nd(NO_3)_3 \cdot 6H_2O$ was mixed with 2.0 g of DMF and 2.2 g of ethanol. The two mixtures were under magnetic stirring at room temperature for 30 min. Then, the solution was added into 0.5 g of PVP and kept stirring for 12 h. The mixture was ejected from the stainless steel capillary with a voltage of 13 kV. The distance between the capillary and collector was 25 cm. Then the electrospinning non-woven mats were collected and annealed with a rising rate of 17 °C/min from room temperature and a keeping time of 120 min at 550 °C.

Structure analysis by X-ray diffraction (XRD) was conducted on a PANalytical B.V. Empyrean X-ray diffractometer with Cu Kα radiation (λ = 0.15406 nm). Scanning electron microscopy (SEM) images were performed on a Hitachi S-4800 instrument. Energy-dispersive X-ray (EDX) spectrometry was performed using a Hitachi S-4800 system.

2.2. Fabrication and measurement of sensors

The process of gas sensor fabrication is described in previous works [23]. Briefly, a certain volume of deionized water was mixed with the samples to form a paste and then the paste were coated on a pair of gold electrodes. The gas-sensing properties of sensors were measured using a CGS-8 intelligent gas-sensing analysis system (Beijing Elite Tech Co., Ltd., Beijing, China). In a testing process, the sensors were pre-heated at different operating temperatures until the resistances of all the sensors were steady. Subsequently, saturated target vapor was injected into a test chamber (about 3 L volume) by a microinjector through a rubber plug. The saturated target gas was mixed with air (relative humidity was about 25% and room temperature was about 25) by two fans in the analysis system. After the sensors resistances reached a new constant value, the test chamber was opened to expose the sensors in air. All the measurements were performed in a laboratory fume hood. The sensors resistance and response values were acquired by the analysis system automatically.

The ratio of the sensor resistances in air (R_a) to that in target gas (R_g) is defined as the sensor response ($S = R_a/R_g$). The response time was defined as the time taken by the sensor to achieve 90% of the resistance variation, and the recovery time was the time taken by the sensor to return 90% of the resistance variation when exposed to air.

3. Results and discussion

3.1. Structure and morphological characteristics

Fig. 1 shows the X-ray diffraction (XRD) patterns of pure and Nd-doped porous In_2O_3 nanotubes. As shown in the picture, all the samples are well-crystallized, the diffraction peaks can be indexed to cubic In_2O_3 (JCPDS No. 71-2195). All the samples were of high purity as no additional impurity peaks are detected.

Fig. 2 shows the energy-dispersive X-ray (EDX) patterns collected from (a) pure and (b) Nd-doped In_2O_3 porous nanotubes. It can be seen from the comparison of the two figures that Nd has been successfully doped. The insert tables reveals the doping level of Nd. The peak of C is derived from the conducting resin during the measurement.

Fig. 3 displays the morphologies of pure and Nd-doped In_2O_3 porous nanotubes. As shown in the picture, all the porous nanotubes are oriented randomly and there are visible pores with
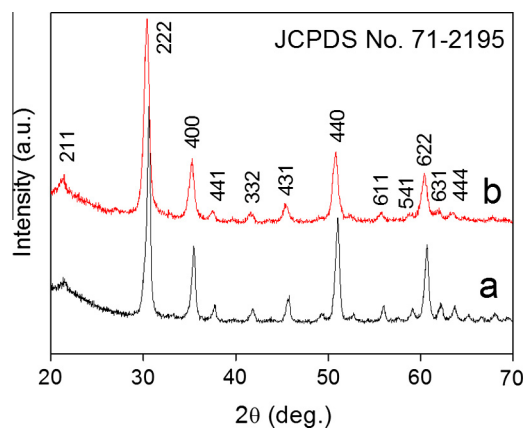

Fig. 1. XRD patterns of (a) pure and (b) Nd-doped porous In_2O_3 nanotubes.

uniform size distributed on the surface, which provides convenient access for gas diffusion into the entire nanotubes.

3.2. Gas-sensing properties

For such semiconducting oxide sensors, there exits an optimum operating temperature. Aiming to find the optimum operating temperature, we tested the pure and Nd-doped porous In_2O_3 nanotube sensors under a variation of temperatures ranged from 200 °C to 280 °C. As shown in Fig. 4, the sensitivity value rises sharply as the temperature and reaches the maximum of 44.6 at 240 °C. Then, the sensitivity declines when the temperature continues increasing. Therefore we defined 240 °C as the optimum operating temperature and the followed examinations of gas-sensing properties are taken under 240 °C. It can be seen from the dynamic response curves that the sensors show fast response and recovery speeds at different temperatures. Moreover, it can be seen that compared with pure In_2O_3 porous nanotubes, Nd-doped In_2O_3 porous nanotube gas sensors exhibit better gas-sensing performance, which is 3.6 times larger than that of pure In_2O_3 porous nanotubes.

Fig. 5 shows the response fitting curves of Nd-doped In_2O_3 porous nanotubes to different concentrations of formaldehyde at 240 °C. The obtained results show exponent curve in general and the fitting parameter of R^2 is 0.98824. The response curve has not saturated until 3000 ppm, indicating a broad measurement scope of such sensors. The insert image presents the linear fitting curve at low concentrations and the fitting parameter of R is 0.9955. The response to 20, 50 and 100 ppm of formaldehyde are about 7.4, 24.5 and 44.6, respectively. Furthermore, the lowest detection limit concentration is also worth noting in practical applications. The response of Nd-doped In_2O_3 porous nanotube gas sensor to 100 ppb formaldehyde is 2.2 at 240 °C. The excellent formaldehyde-sensing performances indicate the as-synthesized materials are promising candidates for practical applications as gas sensors.

Table 1 displays the comparison of sensing performance with previous reports. It can be seen that the performance of porous Nd-doped In_2O_3 nanotube sensors has improved compared to previous works.

Response and recovery speeds are important attributes of gas sensors, which reflecting the repeatability and stability of sensors. Fig. 6 shows four dynamic response and recovery curves of Nd-doped In_2O_3 porous nanotubes to 100 ppm of formaldehyde at 240 °C. The response and recovery times are about 15 and 50 s, respectively. The fast response and recovery speed may be due to the excellent porous nanotube structure, which is favorable for oxygen and formaldehyde gas molecules flow through the entire
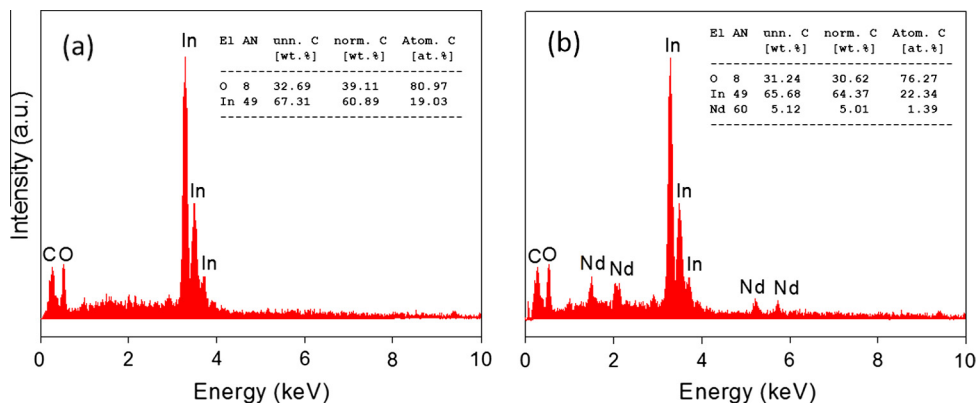
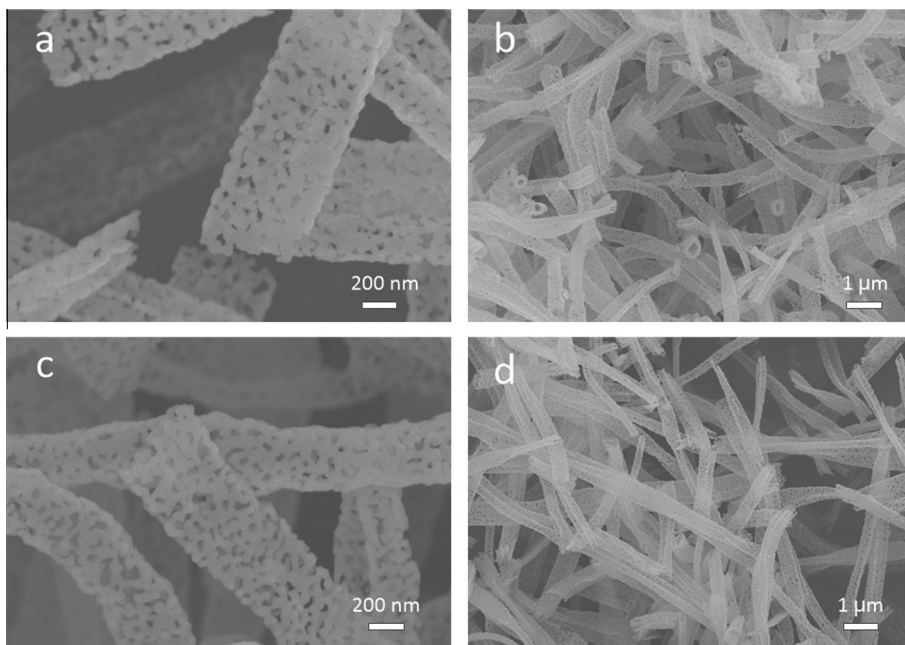**Fig. 2.** EDX patterns of (a) pure and (b) Nd-doped porous In_2O_3 nanotubes.

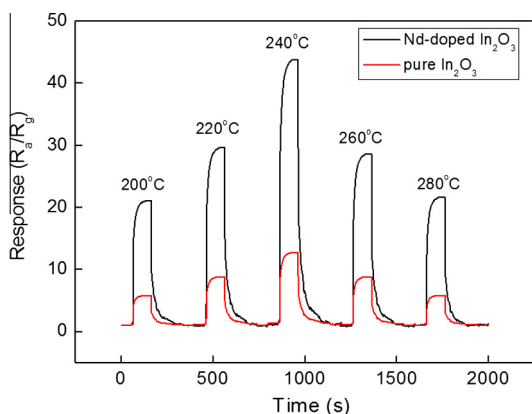**Fig. 3.** SEM images of (a, b) pure and (c, d) Nd-doped porous In_2O_3 nanotubes.

Fig. 4. Responses curves of pure and Nd-doped porous In_2O_3 nanotube sensors to 100 ppm of formaldehyde at different operating temperatures.
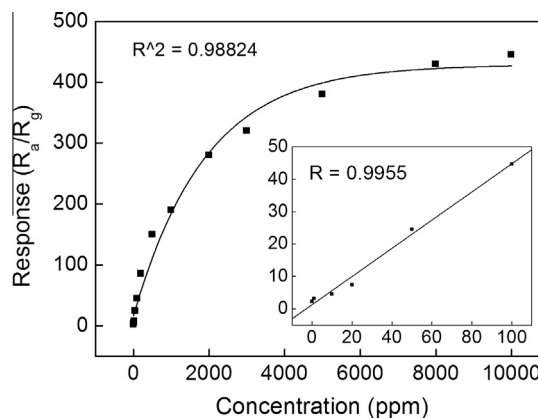

Fig. 5. The response fitting curves of Nd-doped porous In_2O_3 nanotube sensors to different concentrations of formaldehyde at 240 °C (0.1–10 000 ppm). (The insert image presents low concentrations (0.1–100 ppm)).

nanotubes. The sensitivity value and response and recovery speed almost unchanged during the four cycles, indicating the replicability and stability of Nd-doped porous In_2O_3 nanotubes.

In practical applications, sensors are often faced with complex environments of multi gases coexist. So successfully identification

Table 1
Comparison of sensing performance with previous reports.

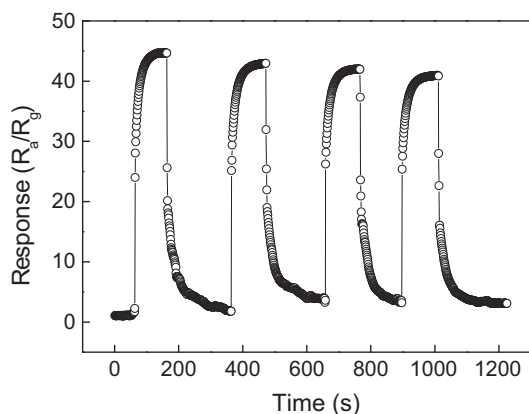| Gas sensors	Sensitivity	Working temperature/°C	Gas concentration/ppm	Response value	Reference
Nd-In$_2$O$_3$	R_a/R_g	240	100	44.6	This work
SnO$_2$ nanospheres	R_a/R_g	260	100	21	[24]
Fe$_2$O$_3$-In$_2$O$_3$	R_a/R_g	250	100	33	[25]
NiO	R_a/R_g	300	100	11	[26]
SnO$_2$-graphene	R_a/R_g	260	100	35	[27]

Fig. 6. The response and recovery curves of Nd-doped porous In$_2$O$_3$ nanotube sensors to formaldehyde at 240 °C.

of target gas under interferences is one of the most important properties of gas sensors. During the examination, Nd-doped In$_2$O$_3$ porous nanotube gas sensors are tested to 100 ppm of different gases and the results are shown in Fig. 7. From the picture, it can be seen that Nd-doped In$_2$O$_3$ porous nanotubes show lower sensitivity to some common gases including ethanol, butane, ammonia, carbon monoxide, hydrogen and toluene. The response values of different gases are different at the same operating temperature, which may be caused by the characteristics of materials. Previous studies have demonstrated that the same sensor can be used to detect different gases by setting different operating temperatures. The energies of adsorption, desorption and reaction on materials for different gases are different, so that the response values are different at the same operating temperature [28,29].

Fig. 8 displays the sensitivity of porous Nd-doped In$_2$O$_3$ nanotube sensors to 20, 50 and 100 ppm formaldehyde within 20 days. It can be seen that the response of gas sensors remained stable
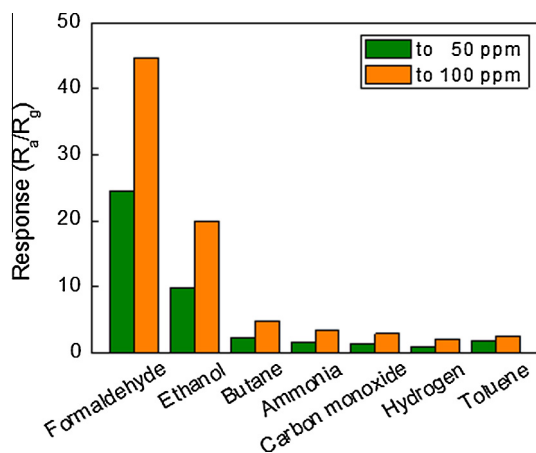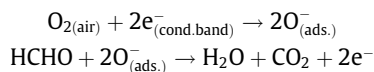
generally during the test, demonstrating the long-term stability of porous Nd-doped In$_2$O$_3$ nanotube sensors.

3.3. Gas-sensing mechanisms of Nd-doped In$_2$O$_3$ porous nanotubes

The major gas-sensing principles of semiconducting oxides sensors can be interpreted as the adsorption and desorption of gas molecules on the surface of materials [25]. In brief, when a sensor is in air environment, O$_2$ will adsorb on the surface of In$_2$O$_3$ and capture electrons from the materials. Then, the adsorbed O$_2$ will convert to O$^-$. This process leads to the decrease of electron density in the conduction band and the increase of material resistance. However, when a reducing gas such as formaldehyde is introduced, formaldehyde gas molecules will react with the absorbed oxygen species and forming CO$_2$ and H$_2$O. At the same time the reaction releases electrons into the conduction band. As a result an obvious change of resistance is observed. The reaction can be described as the following formula [30],

$$O_{2(air)} + 2e^-_{(cond.band)} \rightarrow 2O^-_{(ads.)}$$
$$HCHO + 2O^-_{(ads.)} \rightarrow H_2O + CO_2 + 2e^-$$

In addition, the unique porous nanotube structure helps improve the gas-sensing performance of In$_2$O$_3$. Many studies have demonstrated that the exposure of the inner/outer surfaces of nanotubes will provide larger reactive sites, which is very crucial for their gas-sensing performance. The porous nanotube structure is a more open nanostructure that provides more convenient channels for the penetration of gas molecules to the whole nanotubes. Moreover, because of the pores on the surface offer more sufficient contact and reaction sites, the reaction between the adsorbed oxygen species and the target gas become more violent, which leading to an enhancement of gas sensitivity [31].

The Nd dopant plays another important role in terms of improving the gas sensing performances. In$_2$O$_3$ is an n-type semiconducting oxide [32], while Nd$_2$O$_3$ is a p-type semiconducting oxide [33].

Fig. 7. The responses of Nd-doped porous In$_2$O$_3$ nanotube sensors to different gases at 240 °C.
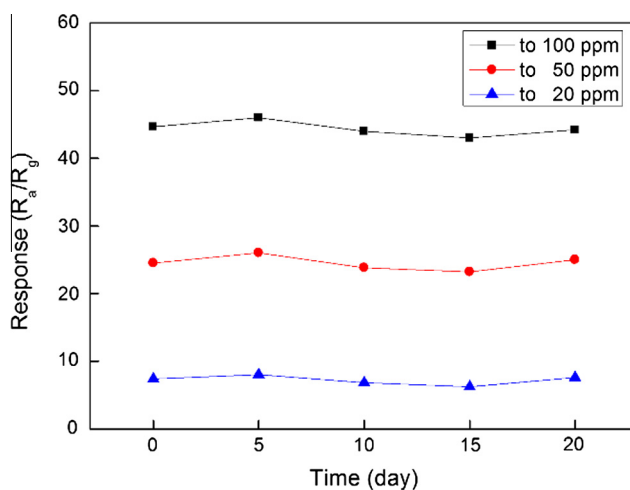

Fig. 8. Long-term stability of porous Nd-doped In$_2$O$_3$ nanotube sensors.

When two semiconducting metal oxides having different Fermi levels contact with each other, a heterojunction will be formed at the interface of them. Electrons move from the n-type In_2O_3 to p-type Nd_2O_3 while vacancies move from p-type Nd_2O_3 to n-type In_2O_3. At last the two oxides achieve equal status of Fermi level, at the same time a junction depletion layer which hinders electron transport formed at the junction [34]. As a result, the resistance in air (R_a) of Nd-doped In_2O_3 porous nanotubes increases significantly. However, when a reducing gas such as formaldehyde is introduced, the adsorbed oxygen will interact with formaldehyde gas molecules and this process will release electrons into the conduction band of materials. Therefore the depletion layer contracts and the conductivity in target gas (R_g) of Nd-doped In_2O_3 porous nanotubes increases [35]. Thus the sensitivity (R_a/R_g) of In_2O_3 porous nanotubes has been enhanced after incorporated after doping with Nd.

4. Conclusion

In summary, pure and Nd-doped In_2O_3 porous nanotubes were successfully synthesized via the electrospinning method. The formaldehyde sensing properties were investigated which indicating doping Nd to be an efficient method of enhancing the formaldehyde sensing properties of porous In_2O_3 nanotubes. The optimum operating temperature for Nd-doped In_2O_3 porous nanotubes is 240 °C. At 240 °C the response of Nd-doped In_2O_3 porous nanotube gas sensors is 44.6 to 100 ppm formaldehyde, which is 3.6 times larger than that of pure In_2O_3 porous nanotubes (12.5). The response and recovery times of Nd-doped In_2O_3 to 100 ppm formaldehyde are 15 and 50 s, respectively. Moreover, the lowest detecting limit is 100 ppb with a value of 2.2. Furthermore, the Nd-doped In_2O_3 porous nanotubes exhibit excellent selectivity to formaldehyde. These advantages indicate the as-prepared Nd-doped In_2O_3 porous nanotubes can be used as a promising candidate for gas sensors in practical applications.

Acknowledgments

References

[1] Y. Li, J. Wu, N. Chopra, Nano-carbon-based hybrids and heterostructures: progress in growth and application for lithium-ion batteries, J. Mater. Sci. 50 (2015) 7843–7865.

[2] R. Timor, H. Weitman, N. Waiskopf, U. Banin, B. Ehrenberg, PEG-phospholipids coated quantum rods as amplifiers of the photosensitization process by FRET, ACS Appl. Mater. Interfaces 7 (2015) 21107–21114.

[3] H.P. Hong, J.H. Kim, C.J. Lee, N.K. Min, In-plane impedancemetric ammonia sensing of solution-deposited, highly semiconductor-enriched single-wall carbon nanotube submonolayer network gas sensors, Sens. Actuat. B – Chem. 220 (2015) 27–32.

[4] X. Pan, X. Zhao, Ultra-high sensitivity zinc oxide nanocombs for on-chip room temperature carbon monoxide sensing, Sensors 15 (2015) 8919–8930.

[5] F. Fang, L. Bai, H. Sun, Y. Kuang, X. Sun, T. Shi, et al., Hierarchically porous indium oxide nanolamellas with ten-parts-per-billion-level formaldehyde-sensing performance, Sens. Actuat. B – Chem. 206 (2015) 714–720.

[6] E.V. Sokovykh, L.P. Oleksenko, N.P. Maksymovych, I.P. Matushko, Influence of temperature conditions of forming nanosized SnO_2-based materials on hydrogen sensor properties, J. Therm. Anal. Calorim. 121 (2015) 1159–1165.

[7] Y. Wang, B. Liu, S. Xiao, H. Li, L. Wang, D. Cai, et al., High performance and negative temperature coefficient of low temperature hydrogen gas sensors using palladium decorated tungsten oxide, J. Mater. Chem. A 3 (2015) 1317–1324.

[8] A. Rydosz, A. Szkudlarek, Gas-sensing performance of M-doped CuO-based thin films working at different temperatures upon exposure to propane, Sensors 15 (2015) 20069–20085.

[9] L. Ma, J.-M. Zhang, K.-W. Xu, V. Ji, A first-principles study on gas sensing properties of graphene and Pd-doped graphene, Appl. Surf. Sci. 343 (2015) 121–127.

[10] B. Huang, C. Zhao, M. Zhang, Z. Zhang, E. Xie, J. Zhou, et al., Doping effect of In_2O_3 on structural and ethanol-sensing characteristics of ZnO nanotubes fabricated by electrospinning, Appl. Surf. Sci. 349 (2015) 615–621.

[11] D. Han, P. Song, S. Zhang, H. Zhang, Q. Xu, Q. Wang, Enhanced methanol gas-sensing performance of Ce-doped In_2O_3 porous nanospheres prepared by hydrothermal method, Sens. Actuat. B – Chem. 216 (2015) 488–496.

[12] N. Mitoma, S. Aikawa, X. Gao, T. Kizu, M. Shimizu, M.-F. Lin, et al., Stable amorphous In_2O_3-based thin-film transistors by incorporating SiO_2 to suppress oxygen vacancies, Appl. Phys. Lett. 104 (2014) 102103.

[13] S. Wang, Z. Li, P. Wang, C. Xiao, R. Zhao, B. Xiao, et al., Facile synthesis and enhanced gas sensing properties of In_2O_3 nanoparticle-decorated ZnO hierarchical architectures, CrystEngComm 16 (2014) 5716.

[14] X. Liang, T.-H. Kim, J.-W. Yoon, C.-H. Kwak, J.-H. Lee, Ultrasensitive and ultraselective detection of H_2S using electrospun CuO-loaded In_2O_3 nanofiber sensors assisted by pulse heating, Sens. Actuat. B – Chem. 209 (2015) 934–942.

[15] X. Li, S. Yao, J. Liu, P. Sun, Y. Sun, Y. Gao, et al., Vitamin C-assisted synthesis and gas sensing properties of coaxial In_2O_3 nanorod bundles, Sens. Actuat. B – Chem. 220 (2015) 68–74.

[16] C. Zhao, B. Huang, E. Xie, J. Zhou, Z. Zhang, Improving gas-sensing properties of electrospun In_2O_3 nanotubes by Mg acceptor doping, Sens. Actuat. B – Chem. 207 (2015) 313–320.

[17] M. Tiemann, Porous metal oxides as gas sensors, Chemistry 13 (2007) 8376–8388.

[18] Z. Zhang, Z. Wen, Z. Ye, L. Zhu, Gas sensors based on ultrathin porous Co_3O_4 nanosheets to detect acetone at low temperature, RSC Adv. 5 (2015) 59976–59982.

[19] S. Shao, H. Wu, S. Wang, Q. Hong, R. Koehn, T. Wu, et al., Highly crystalline and ordered nanoporous SnO_2 thin films with enhanced acetone sensing property at room temperature, J. Mater. Chem. C 3 (2015) 10819–10829.

[20] J. Liu, W. Guo, F. Qu, C. Feng, C. Li, L. Zhu, et al., V-doped In_2O_3 nanofibers for H_2S detection at low temperature, Ceram. Int. 40 (2014) 6685–6689.

[21] J. Gao, L. Wang, K. Kan, S. Xu, L. jing, S. Liu, et al., One-step synthesis of mesoporous Al_2O_3–In_2O_3 nanofibres with remarkable gas-sensing performance to NO_x at room temperature, J. Mater. Chem. A 2 (2014) 949–956.

[22] L. Xu, B. Dong, Y. Wang, X. Bai, J. Chen, Q. Liu, et al., Porous In_2O_3: RE (RE = Gd, Tb, Dy, Ho, Er, Tm, Yb) nanotubes: electrospinning prepration and room gas-sensing properties, J. Phys. Chem. C 114 (2010) 9089–9095.

[23] L. Liu, C. Liu, S. Li, L. Wang, H. Shan, X. Zhang, et al., Honeycombed SnO_2 with ultra sensitive properties to H2, Sens. Actuat. B – Chem. 177 (2013) 893–897.

[24] Z. Li, Q. Zhao, W. Fan, J. Zhan, Porous SnO_2 nanospheres as sensitive gas sensors for volatile organic compounds detection, Nanoscale 3 (2011) 1646–1652.

[25] X. Chi, C. Liu, L. Liu, S. Li, H. Li, X. Zhang, et al., Enhanced formaldehyde-sensing properties of mixed Fe_2O_3–In_2O_3 nanotubes, Mater. Sci. Semicond. Process. 18 (2014) 160–164.

[26] X. Lai, G. Shen, P. Xue, B. Yan, H. Wang, P. Li, et al., Ordered mesoporous NiO with thin pore walls and its enhanced sensing performance for formaldehyde, Nanoscale 7 (2015) 4005–4012.

[27] Y. Cao, Y. Li, D. Jia, J. Xie, Solid-state synthesis of SnO_2–graphene nanocomposite for photocatalysis and formaldehyde gas sensing, RSC Adv. 4 (2014) 46179–46186.

[28] S.T. Navale, D.K. Bandgar, S.R. Nalage, G.D. Khuspe, M.A. Chougule, Y.D. Kolekar, et al., Synthesis of Fe_2O_3 nanoparticles for nitrogen dioxide gas sensing applications, Ceram. Int. 39 (2013) 6453–6460.

[29] W. Zheng, Z. Li, H. Zhang, W. Wang, Y. Wang, C. Wang, Electrospinning route for α-Fe_2O_3 ceramic nanofibers and their gas sensing properties, Mater. Res. Bull. 44 (2009) 1432–1436.

[30] H. Zhang, P. Song, D. Han, Q. Wang, Synthesis and formaldehyde sensing performance of $LaFeO_3$ hollow nanospheres, Phys. E: Low-dimens. Syst. Nanostruct. 63 (2014) 21–26.

[31] H. Shan, C. Liu, L. Liu, J. Zhang, H. Li, Z. Liu, et al., Excellent toluene sensing properties of SnO_2-Fe_2O_3 interconnected nanotubes, ACS Appl. Mater. Interfaces 5 (2013) 6376–6380.

[32] D. Braun, V. Scherer, C. Janowitz, Z. Galazka, R. Fornari, R. Manzke, In-gap states of In_2O_3 single crystals investigated by scanning tunneling spectroscopy, Phys. Status Solidi (a) 211 (2014) 59–65.

[33] Gin-ya Adachi, N. Imanaka, The binary rare earth oxides, Chem. Rev. 98 (1998) 1497–1514.

[34] W. Tang, J. Wang, P. Yao, X. Li, Hollow hierarchical SnO_2-ZnO composite nanofibers with heterostructure based on electrospinning method for detecting methanol, Sens. Actuat. B – Chem. 192 (2014) 543–549.

[35] C. Li, C. Feng, F. Qu, J. Liu, L. Zhu, Y. Lin, et al., Electrospun nanofibers of p-type NiO/n-type ZnO heterojunction with different NiO content and its influence on trimethylamine sensing properties, Sens. Actuat. B – Chem. 207 (2015) 90–96.